# HIGH RESOLUTION SATELLITE IMAGES AND LiDAR DATA FOR SMALL-AREA BUILDING EXTRACTION AND POPULATION ESTIMATION

Sathya Ramesh

Thesis Prepared for the Degree of

MASTER OF SCIENCE

UNIVERSITY OF NORTH TEXAS

December 2009

APPROVED:

Pinliang Dong, Major Professor
Xiaohui Yuan, Minor Professor
Chetan Tiwari, Committee Member
Paul Hudak, Chair of the Department of Geography
Michael Monticino, Dean of the Robert B. Toulouse School of Graduate Studies

Ramesh, Sathya. High Resolution Satellite Images and LiDAR Data for Small-Area Building Extraction and Population Estimation. Master of Science (Applied Geography), December 2009, 48 pp., 4 tables, 15 illustrations, references, 46 titles.

Population estimation in inter-censual years has many important applications. In this research, high-resolution pan-sharpened IKONOS image, LiDAR data, and parcel data are used to estimate small-area population in the eastern part of the city of Denton, Texas. Residential buildings are extracted through object-based classification techniques supported by shape indices and spectral signatures. Three population indicators –building count, building volume and building area at block level are derived using spatial joining and zonal statistics in GIS. Linear regression and geographically weighted regression (GWR) models generated using the three variables and the census data are used to estimate population at the census block level. The maximum total estimation accuracy that can be attained by the models is 94.21%. Accuracy assessments suggest that the GWR models outperformed linear regression models due to their better handling of spatial heterogeneity. Models generated from building volume and area gave better results. The models have lower accuracy in both densely populated census blocks and sparsely populated census blocks, which could be partly attributed to the lower accuracy of the LiDAR data used.

ACKNOWLEDGEMENTS

I wish to extend my special thanks to my major professor and supervisor, Dr. Pinliang Dong for his moral support, continual advice, patience and motivation that has greatly enriched my graduate school experience and bring all the ideas to reality. One simply could not wish for a friendlier supervisor. I would like to thank my committee members Dr. Xiaohui Yuan and Dr. Chetan Tiwari for their valuable suggestions and ideas. I would like to thank Dr. Bruce Hunter, Mr. Gary Parker, Mr. Nick Enwright and Mr. Aldo Avino for their technical assistance that helped me work without any interruptions. I am so grateful to all the faculty members and friends in the Department of Geography, University of North Texas for their constant encouragement throughout my graduate studies.

My deepest gratitude goes to my parents Rohini and Ramesh, my sister Sakunthala Prasanna and my brother Sathya Balaji for their unflagging love and support throughout my life. I am indebted to my grandfather, Rajamanickam, for his care and love. Although he is no longer with us, he is forever remembered.

Finally, but most importantly, I would like to dedicate this thesis and my Masters degree to my husband, Prathap Sekaran who listened and discussed ideas about this thesis with me on many occasions. Without his love, encouragement, comfort and inspiration, I could not have accomplished this research.

TABLE OF CONTENTS

LIST OF TABLES

LIST OF ILLUSTRATIONS

# CHAPTER 1

# INTRODUCTION

## Significance of Population Estimation

The distribution of human population has been identified as one of the key datasets for improved understanding of the impacts of human activities on economical and biological sustainability (Christopher et al., 1999). Traditionally, across the world, census data provide information on population numbers and composition in a decennial basis which requires significant human, technological and fiscal resources. The decennial census of US is a depiction of national population on April 1 of the census year. In such rapidly growing nations, the population count in the decennial basis becomes unrepresentative as decade progresses. According to the United States Census Bureau, the city of Denton had a 2008 population estimate of 119,484 and was ranked in the top 25 of the fastest growing cities in the nation. The city of Denton experienced an increase in growth from 2000 to 2008 at a rate of 48.3% compared with county and state rates of 47.0% and 16.7%, respectively.

Modeling detailed small area population provides a key source for various applications including environmental, health and policy domain. Small area is defined as the subdivisions of the primary political divisions of a country. In United States, counties and their subdivisions are usually considered small areas, although some limit the term to sub county areas such as census tracts,

block groups and blocks and those areas that can be aggregated from these basic units.

Estimating population of such small areas at various scales of space and time is a difficult task. Billions of dollars of federal funds are allocated to states and local entities based on population estimates, hence the significance of accurate population estimation.

## Building Extraction

Identifying residential buildings is considered one of the first steps in determining population estimates. Multispectral images provide us with spectral, textural information and other physical characteristics, but fail to include elevation information which is important for building extraction. Using high resolution satellite images along with digital elevation models (DEM), object extraction techniques were used to update the buildings of existing vector database by deriving three dimensional (3D) information from a pair of high resolution images (Koc and Turker, 2005), but it is found to be more complicated and recommended that the fusion with other data sources may reduce complexity in extraction and reconstruction of features (Suveg and Vosselman, 2004).

Extraction of buildings from remotely sensed data has been progressively developed over time especially with the increasing use of ancillary data. There has been a transition to 3D, object-oriented, hierarchical and multi-scale approaches and more attention has been given to object modeling (Baltsavias,

2004). Based on mathematical morphology, Vu et al. (2009) provided a multi-scale solution to extract building features using mathematical morphology incorporating both elevation and multispectral data. The advanced 3D object extraction technique from LiDAR (light detection and ranging) data makes it easy to extract residential buildings from other land use types which lead to a better estimate of population by dwelling count method. Michaelsen et al. (2008) used stereo pairs of high resolution radar images for building extraction.

*Use of Ancillary Data*

The use of elevation data alone or its fusion with other data sources has widely been used in feature extraction (George et al., 2008; Matei et al., 2008) and enhanced promising accuracies have been attained. Aerial images were used along with LiDAR elevation data to delineate residential buildings (Rottensteiner and Briese, 2003; Vosselman et al., 2005). Zeng et al. (2008) and Matei et al. (2008) tried to use just the LiDAR point clouds to discriminate building features from other features. A classification method is applied to extract buildings using multispectral (MS) imagery and laser altimeter data (Haala and Brenner, 1999). Haala and Brenner (1999) also used laser data and 2D ground plan information and obtained 3D reconstructions of buildings. Without using the ground plan information, Maas and Vosselman (1999) generated roof type specific building models with the help of laser altimetry data. LiDAR data is integrated with building footprints to visualize buildings (Alexander et al., 2009).

### *Object Based Classification*

Object oriented classification seemed to have taken a prime position in the building extraction literatures published. Nearest neighbor object based classification is found to produce higher classification accuracy than the per pixel classification accuracy by 20% (Dehvari and Heck, 2009). Stow et al. (2007) tested two object based classification approaches, one based on spatial frequency characteristics of high resolution Quickbird multispectral image and other based on impervious soil sub objects to identify high and low socio-economic status neighborhoods by delineating residential landuses. Gao et al. (2009) investigated the contribution of multi-temporal enhanced vegetation index (EVI) data for the improvement of object-based classification accuracy by using Multispectral Moderate Resolution Imaging Spectral Radiometer (MODIS) data.

## Traditional Methods for Population Estimation

The United States Census Bureau, in cooperation with state partners, provides inter-censal population estimates to support federal fund allocations. To comply, the Census Bureau has developed three principle methods (Hardin et al., 2007): 1) Ratio correlation procedures – using the ratio of symptomatic variable values for adjacent time periods as independent and dependent variables to estimate population. 2) Component-method II procedures – using registration data on births and deaths to estimate net migration with other administrative information. 3) Housing unit method – using the occupancy rate and average household size along with housing stock and flow derived from US

census of Bureau Survey of building permits and demolitions. Regardless of the method, Hardin et al. (2007) identified a few important factors to be considered: 1) the purpose of population estimation, 2) the spatial scale and time period of the estimation location, 3) data availability and collection of any other ancillary data, 4) selection of appropriate regression method.

## Population Estimation using Remote Sensing and GIS

### *Multispectral Image Sources*

As mentioned earlier, remotely sensed images provide alternative opportunities to estimate population in urban and suburban areas where population growth is alarming. Using remotely sensed data for estimating population started in the mid 1950s with the help of aerial photography. The dwelling units were counted from the aerial photographs in Liberia and multiplied by the number of occupants obtained from a ground survey (Porter, 1956). Since then, counting the dwelling units and estimating population based on average household size have been long used using large scale aerial photographs ( Lo, 1986). This method works well for very small areas but when the model is used to estimate population for entire metropolitan region, it requires large number of aerial photographs and is very time consuming.

After the wide availability of remotely sensed data from various platforms, images of various resolutions started to play a vital role in population estimation research. Hardin et al. (2007) summarizes four primary methods to estimate population using remotely sensed data 1) allometric population growth models

based on the measured residential area. 2) the use of dwelling unit type as a surrogate for family size. 3) the use of landuse type as a surrogate for the population density. 4) pixel based approached modeling population density as a function of spectral signatures and other remotely sensed parameters. High resolution aerial photographs are used to count the number of residential units and based on the household size, the population is estimated (Lo, 1986). Using Geographic Information System (GIS) derived road measurements; Qiu et al. (2003) estimated population through regression models. From the literatures studied, regression analysis is found to be an applicable technique when employing remote sensing. Olorunfemi (1984) concluded that the functional relationship between population density and land type is promising and also examined the goodness of the regression models.

Advanced transformed remote sensing variables including spectral, textural and temperature data have also been explored in estimating population (Li and Weng, 2005; Wu et al., 2005; Weber, 1994; Lo, 1995; Harvey, 2002a; Chen, 2002; Andrew et al., 2004). In addition, Harvey (2000) developed an innovative iterated regression procedure defined as dasymetric modeling to improve the predictive power of a regression model based on pixel spectral values. The use of light emission data as a proxy of population distribution and population density has also received growing attention (Briggs et al., 2006). Henderson et al. (1997) used Synthetic Aperture Radar (SAR) data for detecting settlement areas and estimating population. It is understood that so many

parameters obtained from remotely sensed data are used in one way or the other to estimate population by taking into account residential area indicators.

The gap identified in the pool of research works is that multiple remote sensing resources are not being used efficiently for population estimation. Although there are various research papers on using LiDAR data for 3D object extraction and multispectral data being used to estimate population, integration of LiDAR data and high resolution satellite images for building extraction and population estimation remain limited (Zhou et al., 2004; Bork et al., 2007; Chen et al., 2008). Knowing that one research aspect may be an input to other research problem, this research work would attempt to use object based building extraction technique to support population estimation.

## Research Objectives

The research objectives of this thesis are twofold: (1) to develop efficient and effective methods for building extraction from high resolution IKONOS images with the aid of LiDAR data and object-based classification methods; and (2) to evaluate accuracies of population estimation using variables derived from IKONOS, LiDAR, and parcel data through comparison with census 2000 data and generating linear regression and geographically weighted regression (GWR) models.

# CHAPTER 2

# STUDY AREA AND DATA

## Study Area

The study area is located in the eastern part of the city of Denton, Texas (Figure 1). According to the United States Census Bureau estimate, the population of Denton grew a drastic 48% in a 7 years span which named the city as the tenth fastest growing city in US which substantiates the importance on population estimation of such fast growing cities. Table 1 shows the population estimates of 2006 and 2007 for the 15 largest growing cities in US (US Census Bureau). The source substantiates that the city of Denton has a drastic growth of 4.7% in just one year. The area has about 8 census tracts, 30 census block groups and 764 census blocks covering about 132 Sq. Km.

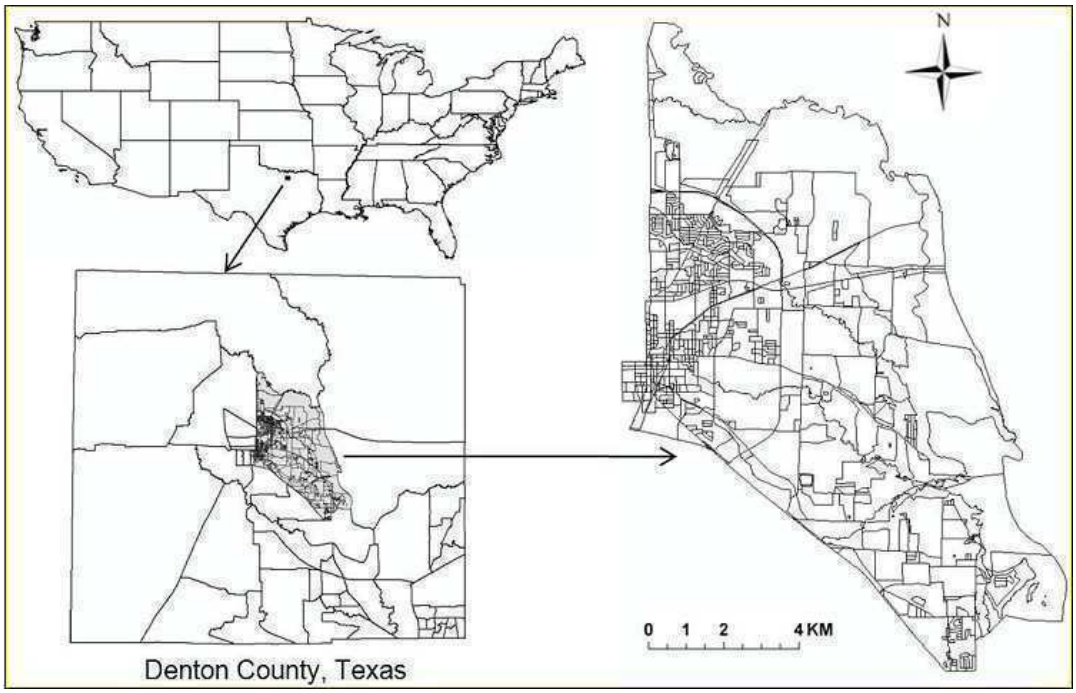


*Figure 1*. Study area: Eastern part of the city of Denton, Texas.

Table 1

*Population Estimates of Growing US Cities*

| Rank | Geographic Area | | Population Estimates | | Change, 2006 to 2007 | |
|---|---|---|---|---|---|---|
| | **Place** | **State** | **1-Jul-07** | **1-Jul-06** | **Number** | **%** |
| 1 | New Orleans city | Louisiana | 239,124 | 210,198 | 28,926 | 13.8 |
| 2 | Victorville city | California | 107,221 | 97,926 | 9,295 | 9.5 |
| 3 | McKinney city | Texas | 115,620 | 107,075 | 8,545 | 8 |
| 4 | North Las Vegas city | Nevada | 212,114 | 197,573 | 14,541 | 7.4 |
| 5 | Cary town | North Carolina | 121,796 | 113,537 | 8,259 | 7.3 |
| 6 | Killeen city | Texas | 112,434 | 105,604 | 6,830 | 6.5 |
| 7 | Port St. Lucie city | Florida | 151,391 | 142,481 | 8,910 | 6.3 |
| 8 | Gilbert town | Arizona | 207,550 | 196,242 | 11,308 | 5.8 |
| 9 | Clarksville city | Tennessee | 119,284 | 113,873 | 5,411 | 4.8 |
| **10** | **Denton City** | **Texas** | **115506** | **110304** | **5202** | **4.7** |

Source: US Census Bureau

## Data

The four datasets (shown in Figure 2) acquired for this study area are:

(1) IKONOS images

(2) Light detection and ranging data (LiDAR)

(3) 2000 census and

(4) Parcel data

### *IKONOS*

The high resolution satellite image used in this research is IKONOS. Developed by Space Imaging, IKONOS was launched September 24, 1999. IKONOS is designed to occupy 682 km sun synchronous orbit at an inclination of 98.1° with 98.3 minutes orbital period. IKONOS empl oys linear array technology and collects data in four multispectral bands including 450nm to 520nm (blue), 510nm to 600nm (green), 630nm to 700nm (red) and 760nm to 850nm (near Infra Red) at a nominal resolution of 4m. It also incorporates a 1-m panchromatic band. The IKONOS image data for this study is acquired on January 3rd 2000, including a 1-m resolution panchromatic band and four 4-m resolution multispectral bands.

### *Light Detection and Ranging (LiDAR) Data*

LiDAR is an active remote sensing technique that revolutionized the acquisition of digital elevation data for large scale mapping applications. A typical LiDAR system is operated from a plane, a helicopter or a satellite. The instrument rapidly transmits pulses of laser which travel to the surface, where they are reflected and the time of pulse return is measured. The return time for each pulse back to the sensor is processed to calculate the variable distances between the sensor and the various surfaces present on the ground (Lillesand, Kiefer and Chipman, 2004). LiDAR data used for this study was acquired on September 4th, 2001. LiDAR Data was collected during leaf-on season and was

post-processed to a point spacing of 3-5 meters. LiDAR data were used to create a DEM and a Digital Surface Model (DSM), which allows for creation of a Normalized Digital Surface Model (nDSM) by subtracting DEM from DSM.

*2000 Census Data and Parcel Data of Denton County*

The 2000 census data is obtained from the US Census Bureau and the parcel data is maintained by the Central Appraisal District of Denton County. The study area consists of about just over 14600 residential, commercial and other land use type parcels.

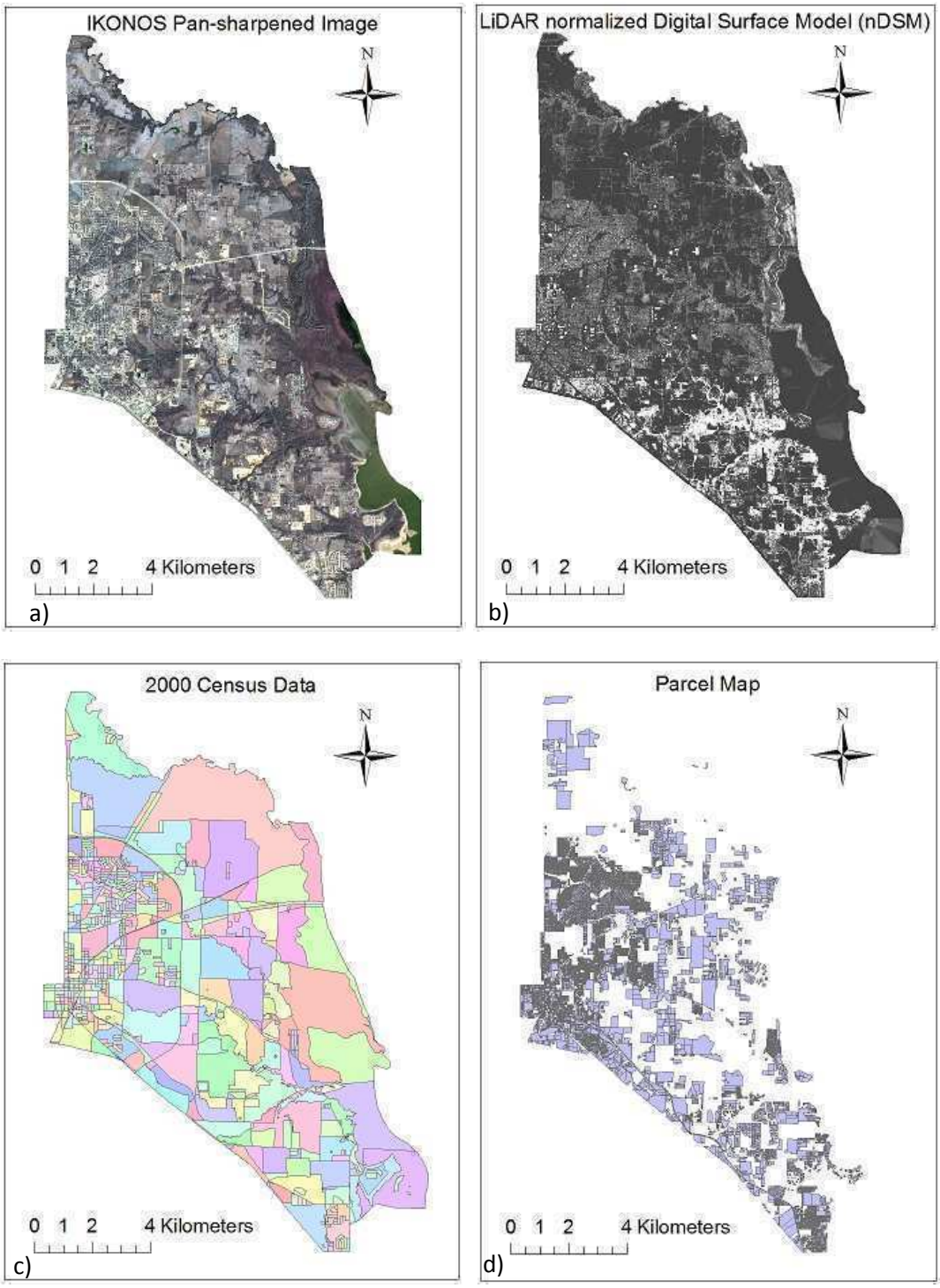


*Figure 2*. Datasets used in the study. a) IKONOS pansharpened b) LiDAR nDSM c) Parcel map d) 2000 census data.

# CHAPTER 3

# METHODOLOGY

A flowchart illustrating the methodology involved in this process is shown in Figure 3. The six major steps involved in the process of estimating population are

(1) Preprocessing LiDAR data

(2) Preprocessing IKONOS data

(3) Object-based classification and extraction of residential buildings

(4) Deriving population indicators, volume of the buildings, area of the buildings and the building count

(5) Regression modeling and

(6) Accuracy assessment.

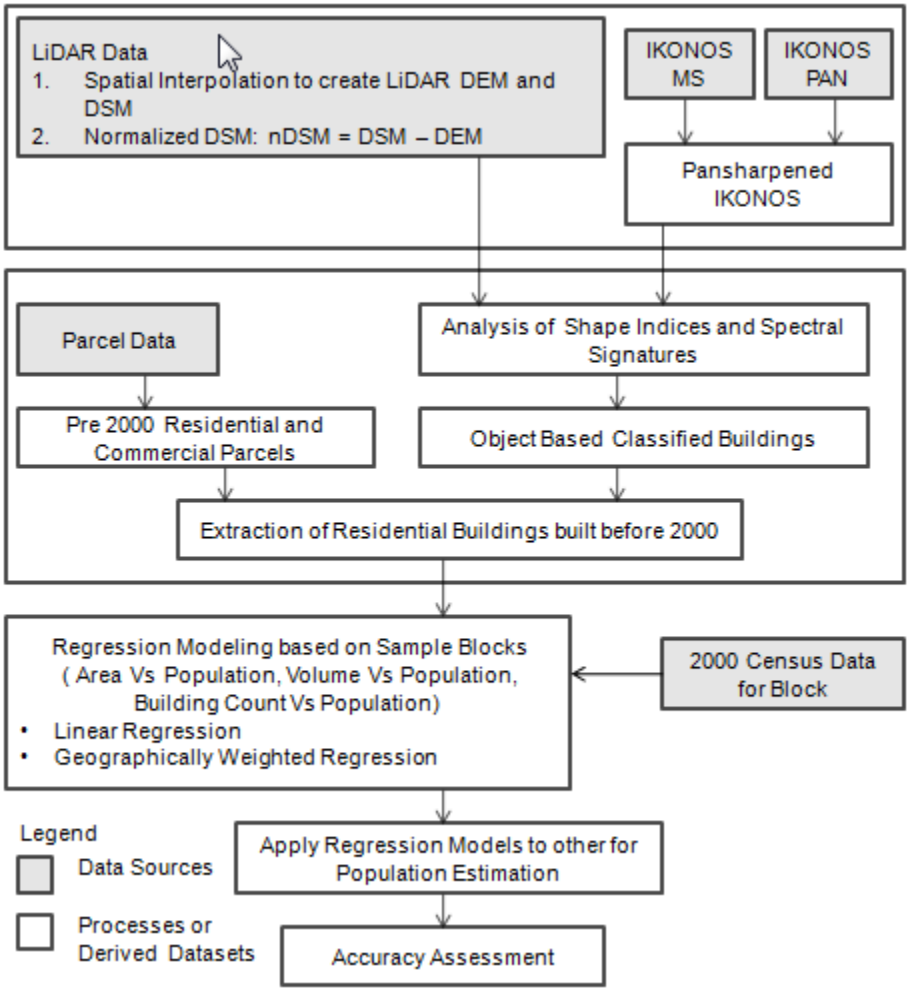


*Figure 3*. Methodology.

## Pre-Processing LiDAR Data

Pre-processing of LiDAR data undergoes a series of steps to derive all the required parameters. The steps are discussed below.

(1) DEM is the digital representation of the ground surface topography or the terrain that provides a so-called bare earth model while DSM includes vegetation, trees, buildings, roads and other features. From the acquired bare earth and reflected LiDAR points, DEMs and DSMs are generated.

(2) The 29 tiles of LiDAR DEMs and DSMs covering the study area are imported to ArcGIS and a point shape file is created. Interpolation is the process by which elevation values of points in geographic space are used to estimate values of positions where elevation information is required. Among various interpolation techniques, Inverse Distance Weight (IDW) interpolation is the simple local method most commonly used (Carter, 1988). IDW is used to interpolate the point shape file to create rasters and all 29 individual tile rasters are mosaiced to create respective DEM and DSM rasters (shown in Figure 4a and 4b). Normalized Digital Surface Model is calculated by subtracting DEM from DSM (Koc and Turker, 2005). Hence, nDSM (shown in Figure 2b) represents the elevation of all the objects and structures present on the surface of the earth including trees, buildings and other man-made objects.

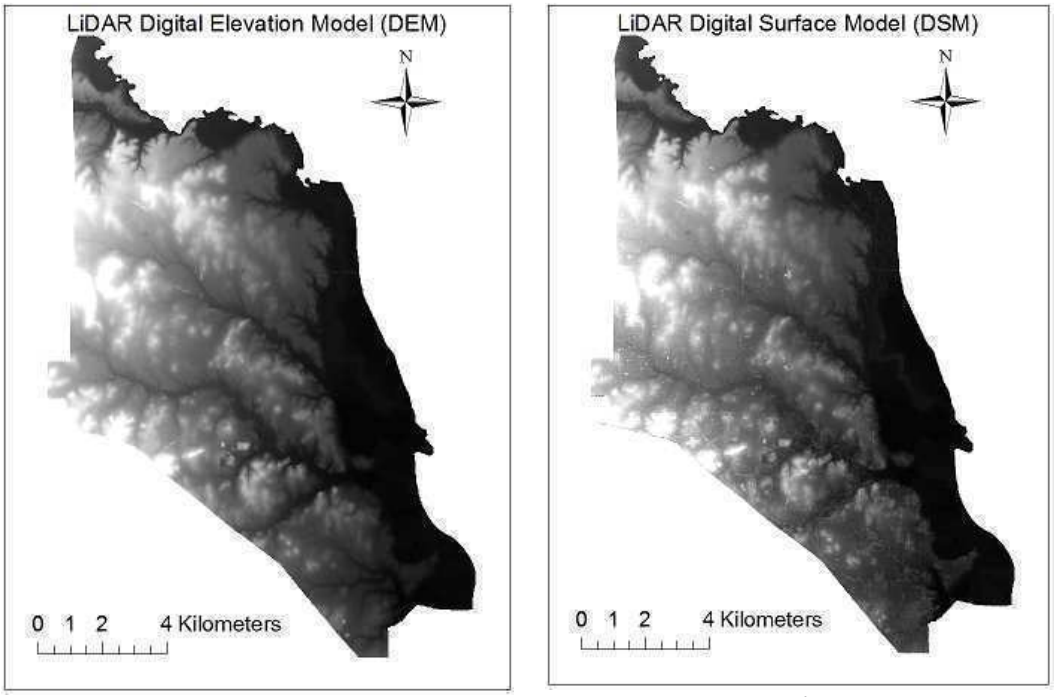


a) b)

*Figure 4*. LiDAR data. a) Digital elevation model (DEM) b) Digital surface model (DSM).

## Pre-Processing IKONOS Data

Efficient building extraction is possible with the availability of high spatial and spectral resolution images. The acquired IKONOS multispectral data has 4-meter spatial resolution while the panchromatic image is a single band image with 1 meter spatial resolution. Image fusion is a concept of combining multiple images into composite products, through which more information than that of individual input images can be revealed. Pan sharpening uses a higher-resolution panchromatic image to fuse with a lower-resolution multiband image.

The most popular image fusion technique in the remote sensing community is the Intensity Hue Saturation (IHS) method. In general, the IHS

fusion method converts a color image from the red, green and blue (RGB) space into the IHS space. The intensity band in the IHS space is replaced by a high resolution Pan image and then transformed back into the original RGB space. IHS method has been preferred over other fusion images because of its fast computing capability and its capability of merging massive volumes of data by requiring only resampled multispectral data. As a preliminary processing, IKONOS MS image is pan sharpened using IHS fusion technique using ESRI's ArcGIS software tool to produce MS image that has the resolution of PAN image. Figure 5 shows the two inputs IKONOS MS and PAN image and the fused image resulting from IHS fusion technique.

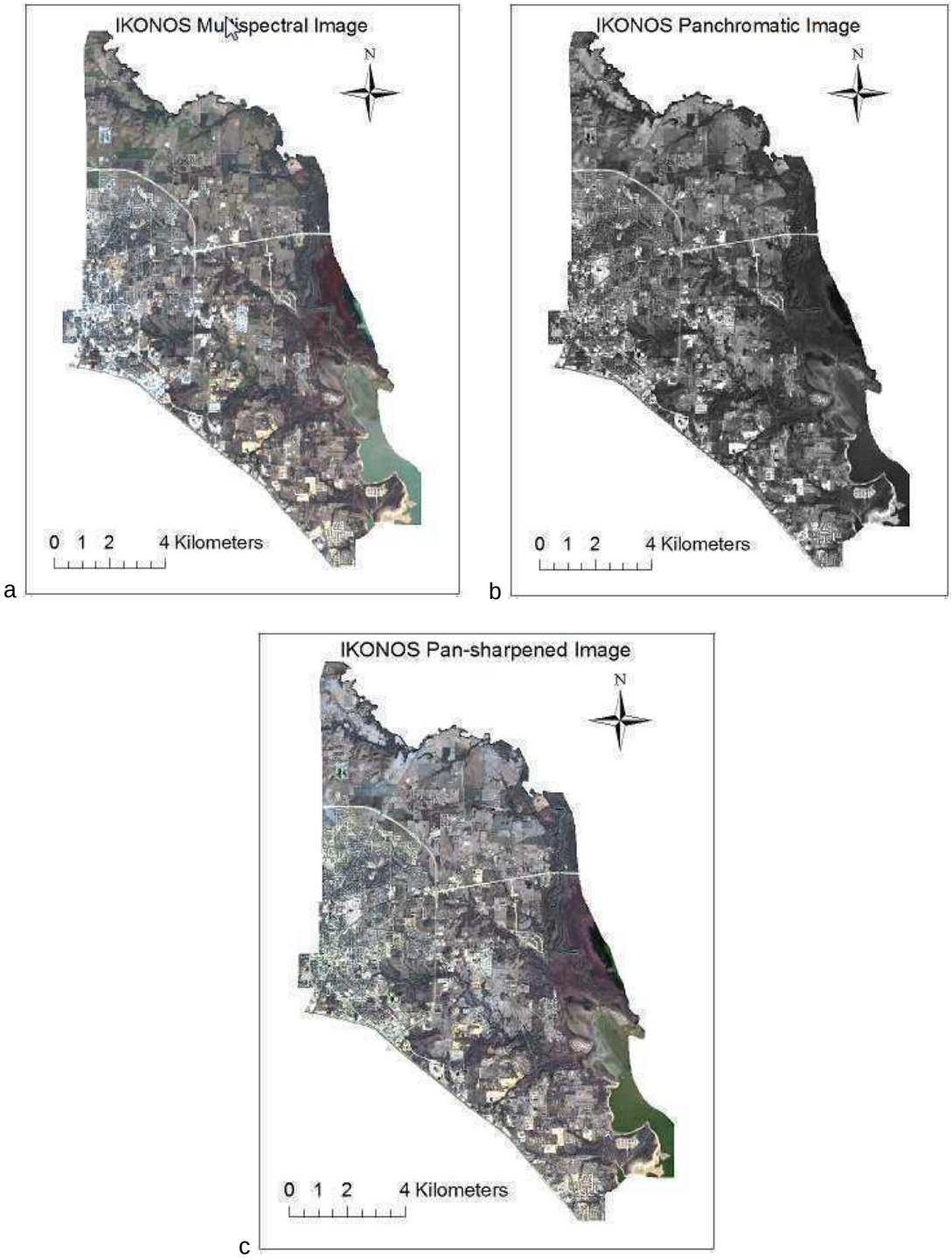


*Figure 5*. IHS fusion. a) Input: IKONOS MS b) Input: IKONOS PAN c) Output: IKONOS pansharpened.

## Object based Classification and Extraction of Building

Remotely sensed data of the Earth may be analyzed to extract useful thematic information. During recent years, the advancement of technology fosters the high availability of high resolution multispectral and hyperspectral data like IKONOS, QUICKBIRD, KOMPSAT, HYPERION, and so on. These datasets promise detailed attribute information but also challenge on methodologies in processing and analyzing them. The classification of land use from high resolution satellite imagery is generally regarded as a difficult task which requires a precise classification methodology. The use of high resolution images in classifying the land cover types that make up the broader class of urban land use is much more difficult. Buildings and roads tend to get lumped together along with parking lots and driveways as impervious areas (Sims and Mesev, 2007).

Traditional per pixel classification methods classifies a pixel identifying its spectral signature as a ground feature. The radiometric value is not related to its neighbor pixels. Though per pixel classifications like maximum likelihood classification are accurate to some degrees, they lack topological information that may result in pepper noise. Object based classification groups neighboring pixels into objects by utilizing the spectral values, topological relationships and also the shape of the objects that are created (Batz et al., 2004). Blaschke (2004) addresses the concepts of object-based image processing in his research considering the contextual information, shape and the spatial relations between the image regions. The combination of object based image classification with

ancillary digital line graph data is proven to improve land cover type classification accuracy (Sims and Mesev, 2007). Object based classification is also attempted on just the LiDAR data to extract features (Antonarakis et al., 2008).

## eCognition and Object based Classification

eCognition software from Definiens offer a similar object oriented classification technique by segmenting the image to meaningful objects. eCognition implements a new segmenting technique called multiresolution segmentation, a bottom up region merging approach. Darwish et al. (2003) tested the feasibility of this classification technique using eCognition software to classify urban land cover in his research. In general, buildings have higher elevation than the surrounding and there will be a steep slope along the edges. Hence, to extract buildings from multispectral image, the stable data is identified as the elevation data. eCognition software is employed in this study to classify high resolution multispectral data, IKONOS with LiDAR elevation data as an ancillary input. This research work aims at attaining higher classification accuracy thereby increasing the accuracy of population estimation model.

In this study, the whole study area is divided into 30 tiles to process the data faster and also to define more specific shape indices. As the study area has mixed topography from low to high density residences and vast farmlands, specifying local height thresholds and shape index thresholds enables to extract buildings more accurately. Two classes, buildings and non-Buildings are

identified using various shape indices mentioned below and general spectral characteristics.

## Shape Indices

Using multiresolution segmentation, the image is divided into meaningful objects. Figure 6 illustrates how image is divided into image objects by image segmentation in eCognition. Each object is then studied for its spectral and shape characteristics to distinguish between the two major classes - buildings and non-Buildings. Trees and other grasslands are removed by using its high vegetative index. Barren lands and other short shrubs are removed from its very low height property. Various shape indices are used to distinguish between building and non building features. Building objects have certain unique characteristics which help us define such indicator parameters. A few indicators and the concept behind the implementation are explained below.

- Area: Area of the polygon is quite useful to differentiate buildings from other objects. Residential buildings are comparatively smaller in size than the large commercial office buildings.
- Asymmetry: The longer a feature polygon, the more asymmetric it is. Residential buildings tend to be more symmetrical. It is hard to see a lengthier residential building. Asymmetry is a measure expressed by the ratio of the lengths of the minor and the major axis of this ellipse.
- Shape Index: It is used to describe the smoothness of the image object borders. Mathematically, Shape Index (SI) can be expressed as:

$$SI = b_v / 4\sqrt{P_v} \quad (1)$$

where $b_v$ is the perimeter of the feature polygon and Pv is the area of the polygon. The denominator represents the largest enclosed circle. The higher the shape index, the more irregular the feature. Hence objects with higher shape index may not be a building.

- Border index: This measure is very similar to shape index other than the use of rectangular approximation instead of a square. The smallest rectangle enclosing the image object is created. The border index is then calculated as the ratio between the perimeter of the image object to the perimeter of the smallest enclosing rectangle.
- Compactness: Compactness of an image object is similar to Border Index, however instead of border based it is area based.
- Rectangular Fit (RF): To calculate the rectangular fit, a rectangle with the same area as the considered object is created by taking into consideration the proportion of the length to the width of the object. The area of the object outside the rectangle is compared with the area inside the rectangle which is not filled with the object. RF is defined as:

$$RF = \frac{\{(x,y) \in P_v : \rho_v(x,y) \leq 1\}}{P_v} \quad (2)$$

where $\rho_v(x,y)$ is the rectangular distance at a pixel (x,y).

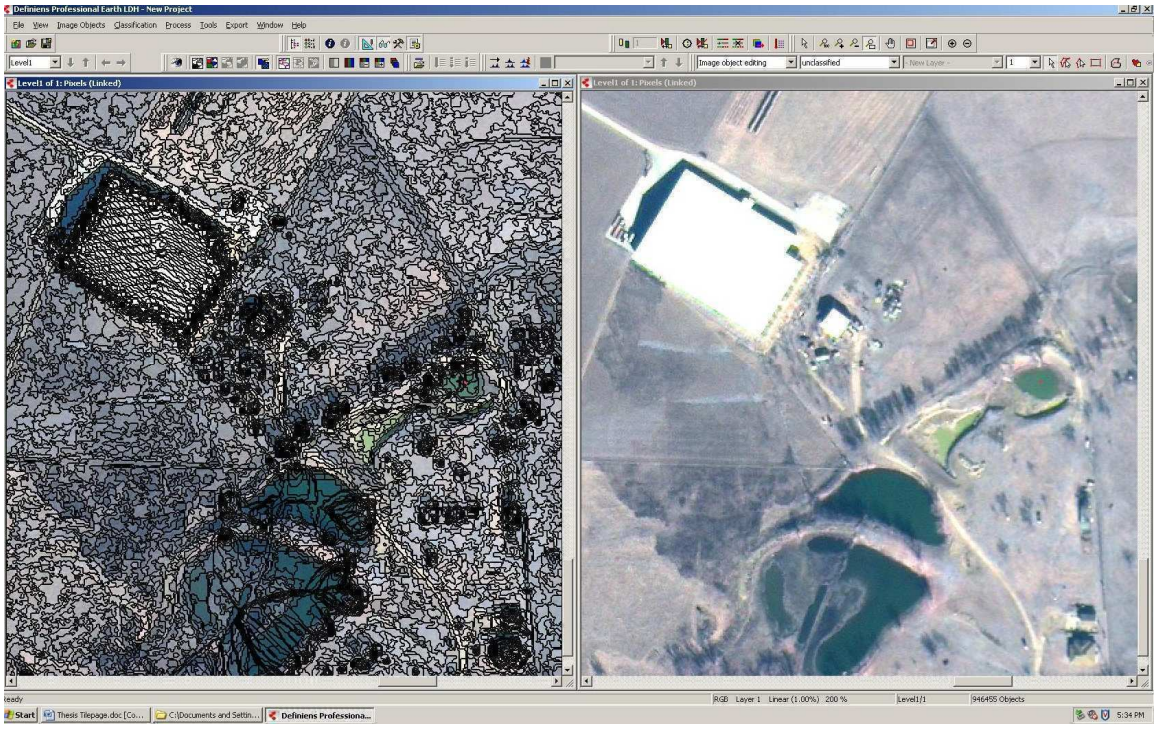

*Figure 6*. Image objects and corresponding IKONOS image.

Residential Building Polygons

The image objects for residential buildings are extracted and exported to a vector shapefile. Using ESRI's ArcGIS software, 30 different building shapefiles obtained from eCognition are merged to a single polygon file that has the residential building information for the entire study area. Since the LiDAR data is acquired on September 2001 which is 17 months after the 2000 census, it is required to remove any new developments built after 2000 from the LiDAR Data. Parcel Data has the information about the land type of each parcel and the property type. Hence, residential and commercial building parcels that are built before 2000 including 2000 is selected from the acquired parcel data and used as a mask to filter the rest of the polygons from the extracted building polygons.

In the parcel data, residential apartment complexes and educational residential buildings are identified as commercial buildings, so commercial parcels are also included in the mask.

## Derivation of the population indicators

The three main population indicators in an urban city are identified as residential building count, residential building area and residential building volume. As this research aims at determining population estimates at the census block level, 2000 census block data is used to generate regression models. The nDSM generated previously and the census block boundaries are used to calculate the residential building area and volume at each block with the help of zonal statistics in ArcGIS. From the building polygons, building centroids are identified and joined with the census block shape file using spatial join. The result of spatial join will give us the building count for each block.

## Regression Modeling

Regression analysis is a statistical tool for the investigation of relationships between variables. It allows us to model, examine, predict and explore spatial relationships and also help explain the factors behind spatial patterns. To perform regression analysis, 95 random blocks are selected as samples from the 2000 census block data These 95 sample blocks distribute across the study area and represent the entire study area which consists of heterogeneous population density and topography. The sample blocks are shown in Figure 7.

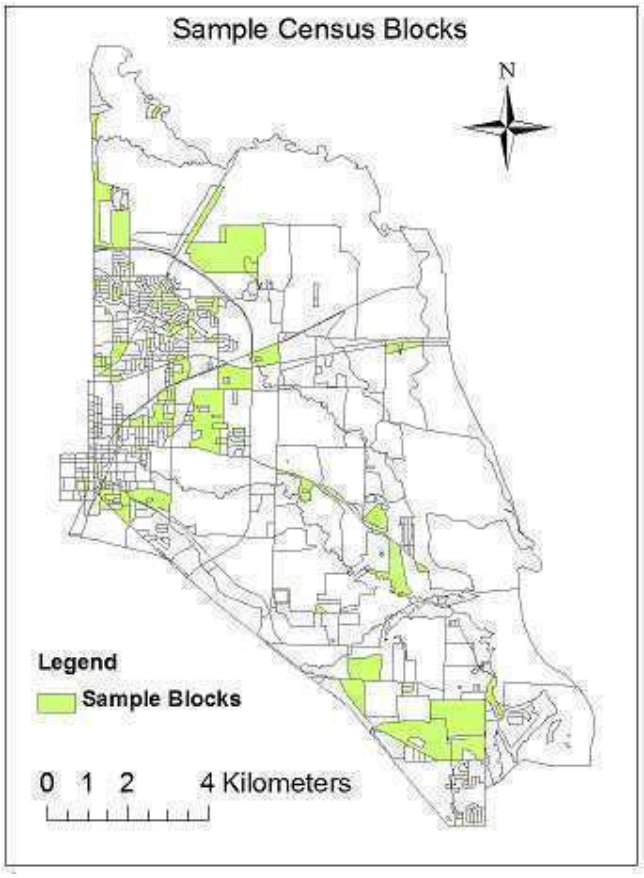


*Figure 7*. Sample census blocks.

Three regression techniques - linear regression, multiple regression and GWR models are used in this study to better model the population. Three linear regression models in the following form are established to estimate population count:

$$PE = a + b \times I \tag{3}$$

where PE is the population estimates, a is the regression intercept, b is the slope and I is the population indicator (residential building area, volume and count). A multiple regression analysis is performed by taking residential building area and

volume as independent variables and population as dependant variables. The regression form is illustrated in the equation shown below.

$$PE = a + b \times BA + c \times BV \ , \qquad (4)$$

where PE is the population estimates, a is the regression intercept, b and c are the slopes of BA (building area) and BV (building volume) respectively.

Geographically Weighted Regression

In a normal regression model, the values a and b in the Equation (3) are considered constants and if there is any geographic variation in the spatial relationship, it will be confined to an error term that resides in the model. GWR is a local version of spatial regression that generates parameters disaggregated by the spatial units of analysis. This allows assessment of the spatial heterogeneity in the estimated relationships between the independent and dependent variables. Hence instead of introducing an error term, GWR tends to include the variability within the model. GWR is increasingly being used in geography and other disciplines recently. Four socio economic variables – median household income, percentage of poverty, percentage of minority population, median house value and their relationships with environmental variables – percent of impervious surface and population density at census block levels are studied using GWR models and is proven that the models account for local effects and geographical variations (Ogneva-Himmelberger et al., 2009). Applying GWR analysis to remotely sensed and statistical data, regression model

is generated to highlight the spatial variation of the relationship between the percentage of land afforested and its proximate causes (Clement et al., 2009).

GWR provides a local model of the variable or process that we are trying to understand by fitting a regression equation to every feature in the dataset. In general, GWR technique constructs a grid of regression points over the study area. A set of regions is then defined around each regression point which is defined as bandwidth. The regression model is then calculated by incorporating the dependent and explanatory variables of features on all the data lying within the region described around a regression point that is weighted by its distance from that regression point and the process is repeated for all regression points. The resulting local parameter estimates can then be mapped at the locations of the regression of the regression points to view possible non-stationary in the relationships examined. Specifying size and shape of the bandwidth is critical and it determines the local models. In some cases, when data are sparse, the local model might be calculated on very few data points, giving rise to parameter estimates with large standard errors and resulting surfaces will be undersmoothed. In the other extreme, the estimation of some parameters might be impossible due to insufficient variation in small samples. In order to reduce these problems, in this study, the spatial bandwidth is made to adapt themselves in size to variations in the density of the data, so that the bandwidth will be larger where the data is sparse and smaller where the data is dense. In this study, ESRI's ArcGIS spatial modeling tool is used to determine an optimal bandwidth

that satisfies least cross validation (CV) score. CV score is determined by the difference between the observed value and the GWR calibrated using the bandwidth.

## Accuracy Assessment

It is vital to substantiate the accuracy of the regression models quantitatively. It is also an important step in estimating population using remote sensing and GIS methods. Similar to Lu et al. (2006), three error measures are used for accuracy assessment.

### *Relative Error (RE)*

Relative error gives an indication of how good a measurement is relative to the actual value being measured.

$$RE = \frac{(P_e - P_g)}{P_g} \times 100, \quad (3)$$

where $P_e$ and $P_g$ are the estimated and reference population in each census block, respectively. Values of RE can be stored in a field in the census block attribute table to support convenient mapping using GIS.

### *Mean Relative Error (MRE)*

Additionally, mean relative error (MRE) can be used to quantify the overall model performance.

$$MRE = \frac{\sum_{k=1}^{n} | RE_k |}{n}, \quad (4)$$

where RE is the Relative Error and n is the total number of census blocks under study.

*Median Relative Error (MdRE)*

Median relative error tends to reduce the influence of extreme outlier values. Hence, median relative error is also calculated and verified in this study.

# CHAPTER 4

# RESULTS AND DISCUSSIONS

Linear and geographically weighted regression models are generated with the help of 2000 Census Block data. The models are applied to the entire 764 blocks and errors are calculated for model accuracies. The results of population estimates are discussed in this section.

## Linear Regression Models

Table 2 shows the errors calibrated for linear regression models with population as a dependant variable and building count, building area and building volume as independent variables respectively.

Table 2

*Summary of Linear Regression Model Results*

| Variable | $R^2$ | Total Error | Mean Error | Median Error | Model |
|---|---|---|---|---|---|
| Count | 0.9521 | -33.3138 | 27.11522 | 20.3986 | y=1.9716x+3.6581 |
| Area | 0.8214 | -21.3202 | 26.59229 | 19.3676 | y=0.0012x+5.6161 |
| Volume | 0.8109 | -5.7925 | 27.27547591 | 17.1896 | y=0.001x+6.744 |

The linear regression models derived from the 95 sampling blocks are represented in Figure 8. Scatter diagrams are generated to better understand the relationships between the relative population estimation errors and population density at each census block and is shown in Figure 9.

The result showing the errors calibrated for multiple regression model specifying population as function of building area and volume is illustrated in Table 3 and the scatter diagrams are illustrated in Figure 10.

Table 3

*Summary of Multiple Regression Model*

| Variable | $R^2$ | Total Error | Mean Error | Median Error | Model |
|---|---|---|---|---|---|
| Area, Volume | 0.8658 | -25.0271 | 26.1185 | 18.5436 | $y=0.0002837x_2 - 0.00001302x_1$ |

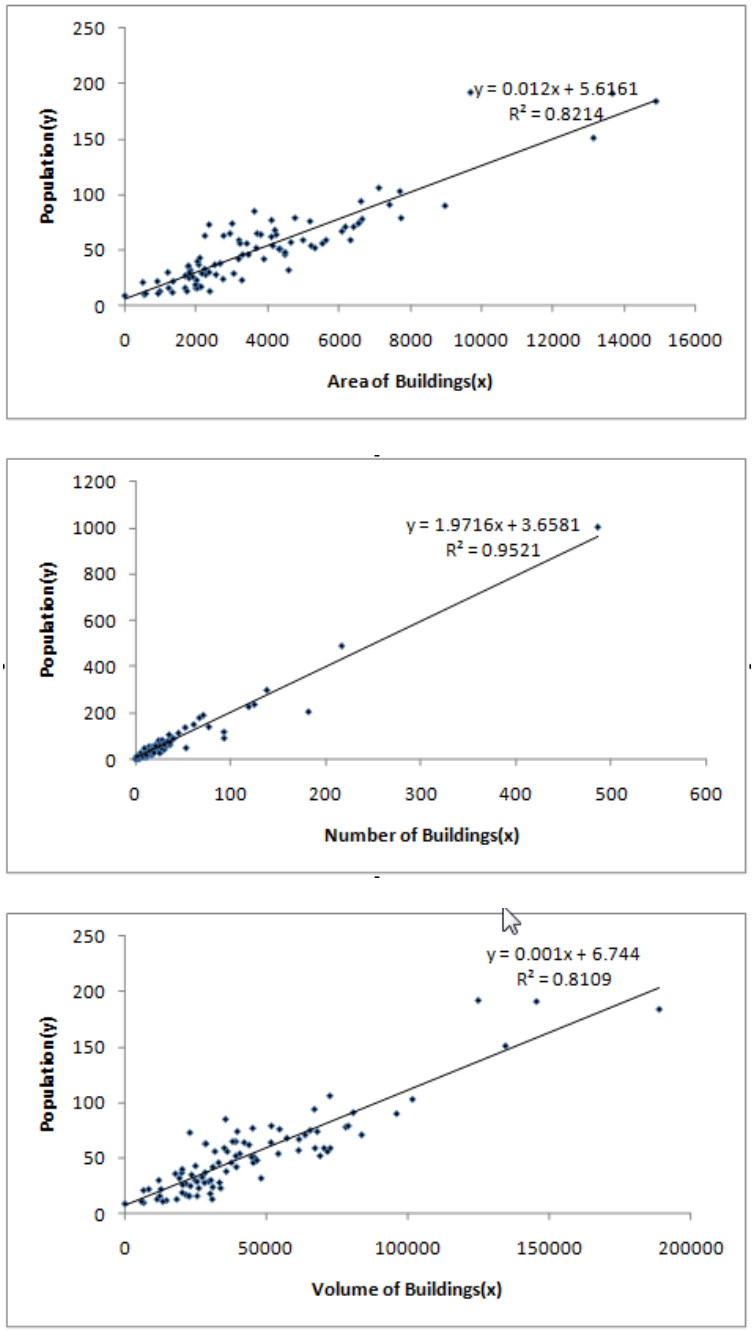


*Figure 8*. Linear regression models derived from sample census blocks.

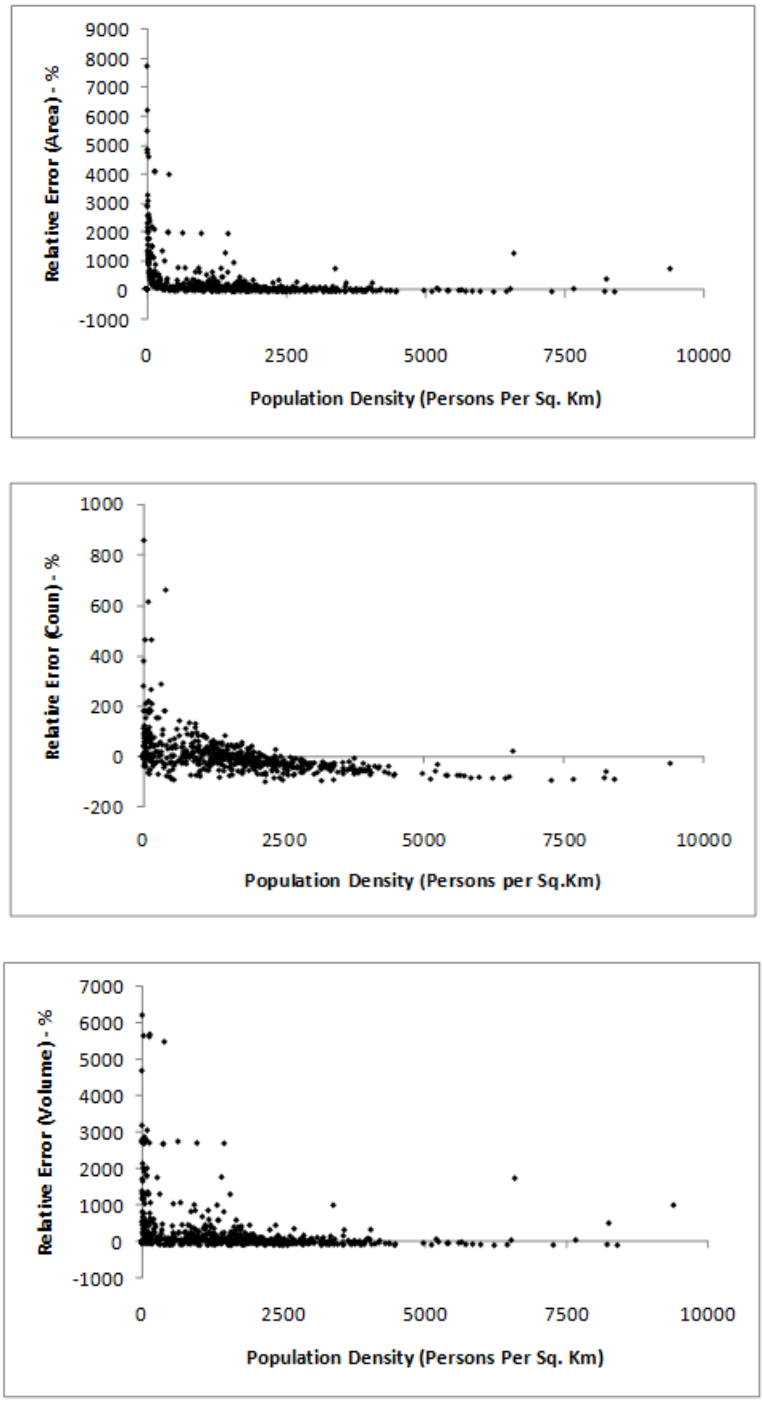


*Figure 9*. Scatter diagrams of relative population estimation error vs. population density for linear regression models.

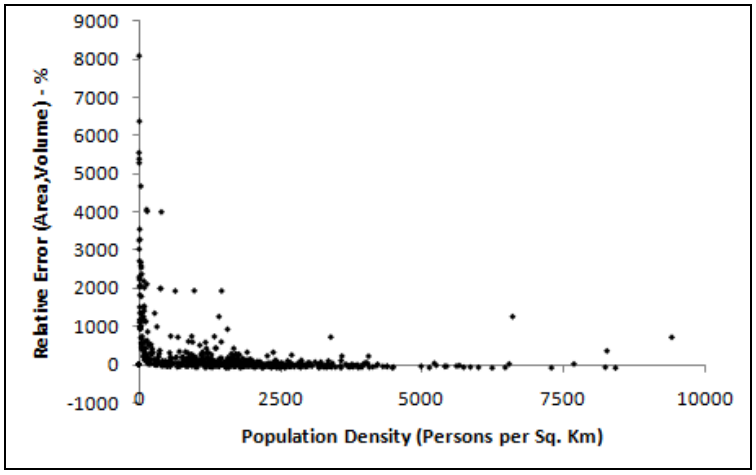


*Figure 10*. Scatter diagram of relative population estimation error vs. population density for multiple regression model.

Geographically Weighted regression

Table 4 shows the errors calculated from the population estimates when geographically weighted regression model is employed to the entire study area. Figure 11 illustrates the scatter diagrams obtained to better understand the relationships between relative population estimation error obtained from GWR models and population density.

Table 4

*Summary of GWR Models Results*

| Variable | R Squared | Total Error | Mean Error | Median Error |
|---|---|---|---|---|
| Count | Local Models | -32 | 25.87057 | 18.43238 |
| Volume | Local Models | -17 | 26.47716 | 13.63282 |
| Area | Local Models | -21 | 36.26646 | 16.46232 |

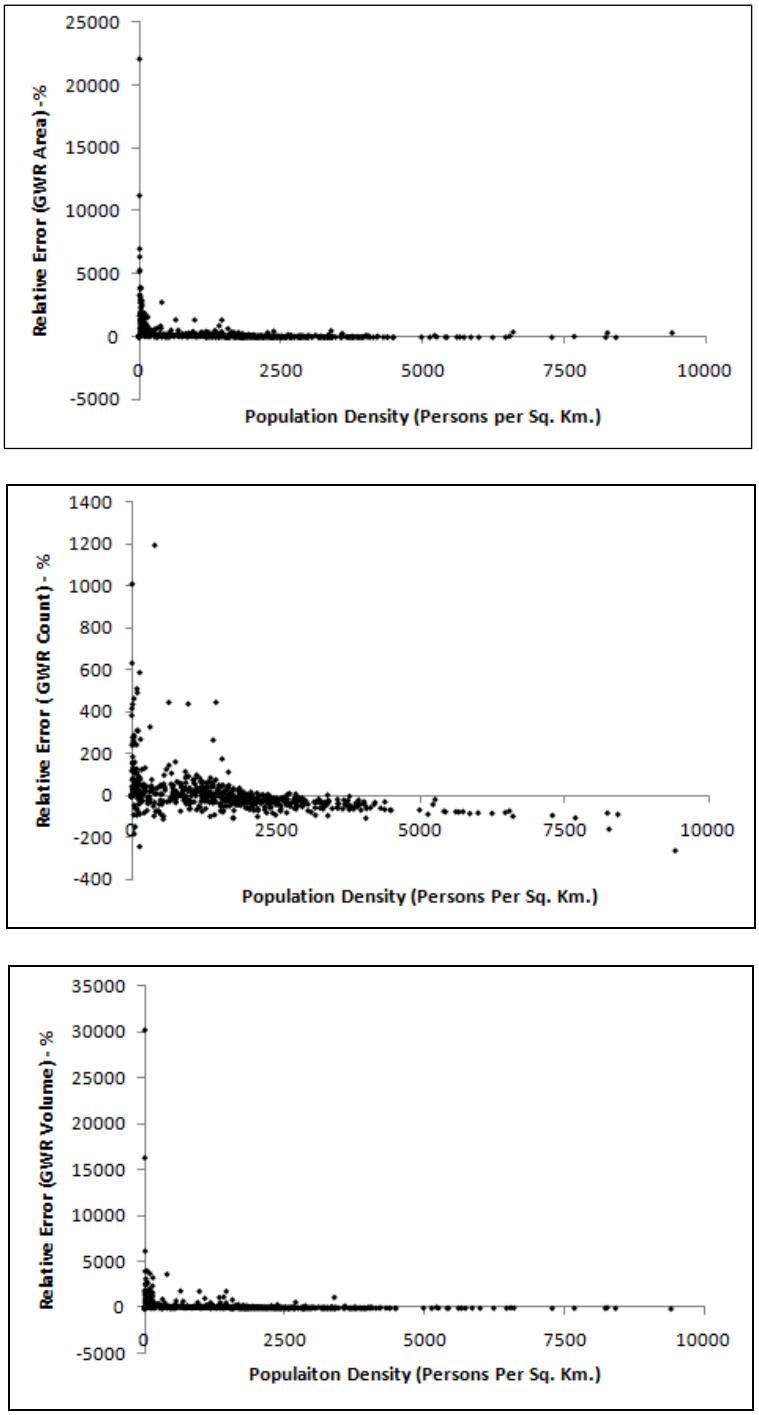


*Figure 11*. Scatter diagram of relative population estimation error vs. population density for GWR model.

A few observations of the above results are discussed in the following section.

1. As far as visually interpreting the image scene, the extracted buildings across the study scene are more accurate. Figure 12 shows a scene from the study area where the buildings are extracted more precisely.

*Figure 12*. Extracted buildings (shown in red outline).

2. However, in a dense residential area (an example is shown in Figure 9), extracting buildings amongst large trees is found to be a difficult task. The LiDAR data in this study were collected during leaf-on season (September 4, 2001) which makes it difficult to separate residential buildings from tree canopies. This may not be a serious problem for relatively new communities where trees are smaller but can be a factor affecting population estimation in older communities with many mature trees as shown in Figure 13b. Figure 13a shows the standard deviation of the original image pixels shown in Figure 13b. By plotting the standard deviation, the slope of the image pixels can be analyzed. In the example figure shown, the three buildings are recognized as trees as the buildings are totally covered. In blocks that has a similar scenario, the number of

building and eventually the building area and volume are underestimated. Hence high resolution LiDAR data is expected to give detailed information and help us do a detailed evaluation for separating trees from buildings based on measures of slope, aspect, and 3D shape and thereby obtain more accurate small area population estimation. A recent study suggests that 3D shape signatures from high resolution LiDAR data can be used to discriminate different tree crowns (Dong, 2009). It is reasonable to expect that 3D shape signatures of buildings and trees can be different, which may help separate trees from buildings.

a) 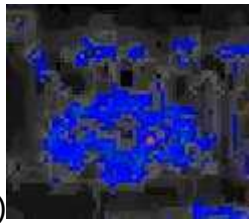 b) 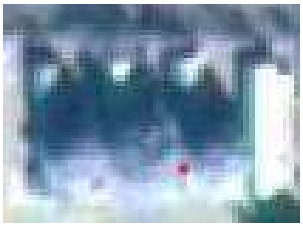

*Figure 13*. Image scene with tree-covered buildings.

Another issue is with differentiating residential buildings from commercial buildings. High rise apartments contradict the general properties of individual houses in terms of shape and size and have high similarity with commercial office buildings. Also, high rise apartments accommodate more number of people and hence small blocks that have few high rise buildings tend to have more population. Such blocks remain as outliers with more relative errors. Separation of high-rise apartment buildings from commercial/industrial buildings using remote sensing remains a challenge. One such sample block is shown in Figure 14. Further study is required to test the use of physical properties of LiDAR

derived buildings and other models of population estimation like kriging (Wu and Murray, 2005).

*Figure 14*. Census block with high rise buildings and huge population (outlined in blue).

3. Temporal component also plays a major role in the estimation errors. The multispectral image is acquired on January of 2000 while the census data is a depiction of population on April 1$^{st}$ 2000. Hence, in those time interval, many new buildings are identified in some blocks whose census population is zero. These buildings are identified as newly built buildings which are vacant but those building count, area and volume are taken into consideration in the model. These vacant buildings are a big problem in such building extraction studies which results in an overestimation of building counts and an example is shown in Figure 15. Block No.0214.015044 is found to have newly constructed buildings but with the census data population as zero.

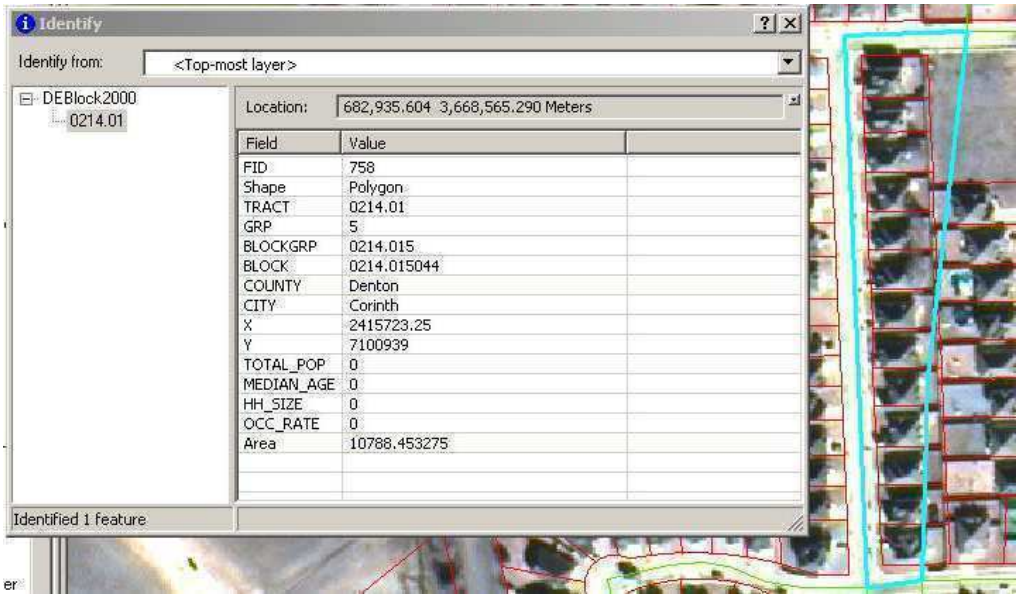


*Figure 15*. Census block having zero population (outlined in blue).

It is observed that the models resulted in a very high mean relative error and relatively low median relative error which indicates of the presence of extreme values as discussed in (2) and (3).

4. The high $R^2$ values for linear and geographically weighted regression models show that the population count is strongly correlated with the residential building count, area and volume derived from IKONOS and LiDAR nDSM. Although some studies show that the Housing Unit method where population estimation is made with the number of building counts offers a number of advantages over other population estimation methods (Smith and Cody, 1994; Smith and Lewis 1980), there is no obvious pattern to show that building count outperformed building area and volume in this study. Moreover, building volume and building area tend to give better median relative estimation errors and total

estimation errors when compared to the building count as shown in Table 1, 2 and 3.

5. Figure 9 and 10 indicates that population estimation is overestimated when the population density at the census block level is less than approximately 300 persons square kilometer, whereas population is underestimated when population density is greater than approximately 3500 persons per kilometers, regardless of the independent variables used in the linear regression models. Similar observations have been reported by Lu et al. (2006) for population estimation using lower multispectral image sources. It is also interesting to see that Figure 10 that shows the relationship between relative estimation errors at block level and population density obtained from the GWR models also infers a very similar scenario where low population density blocks are overestimated and densely populated blocks are underestimated. Total estimation error (TE) is highly influenced by the sign and magnitude of the relative estimation errors. It is observed that underestimation has a larger magnitude because it mainly happens in census blocks with high population density which dominates in the study data. As a result, the total population is underestimated, as illustrated in Tables 1, 2 and 3 irrespective of the variables and models.

6. Values of MdRE in Tables 2, 3 and 4 indicate that the GWR models provide more accurate estimates than the linear regression models because the heterogeneity can be better modeled in GWR models.

7. For census blocks with a low population density (for example, less than 100 persons per Sq. Km), relative error of population estimation in percentage can be highly misleading. For instance, for a census block with actual population of 1 and estimated population of 4, the relative error is 300%, but the actual error of 3 persons may be insignificant compared with the total population of the census tract. Hence small number problems need to be taken into account for population estimation at block level.

8. Overall, the various regression models generated in this study are able to produce 80% to 87% accurate population estimations. The LiDAR data were resampled to a point spacing of 3-5, which affects the accurate representation of buildings. It is possible that the relatively low accuracies for small area population estimation were partly caused by the relative low spatial resolution of the LiDAR data. It would be interesting to compare area-based, volume-based, and count-based linear regression models and GWR models when high resolution LiDAR data are available.

# CHAPTER 5

# CONCLUSION

IKONOS image with high spectral and spatial resolution is generated by fusing IKONOS Panchromatic and IKONOS multispectral images using IHS fusion technique. Object based classification technique is used to extract residential buildings from pan-sharpened IKONOS, normalized digital surface model and parcel map. Using 2000 census data and sample census blocks, linear regression models and GWR models were built from the independent variables of building count, building area, building volume obtained from the extracted buildings. The regression models were then applied to the census blocks in the study area and accuracy assessments were carried out. Models derived from building volume and building area seem to generate more accurate results compared with those derived from building count as area and volume account for living area which is an important indicator of the household size. Median relative errors suggest that the GWR models outperformed the linear regression models because spatial heterogeneity in population density is better handled in GWR models. The results show that the total accuracy of population estimation in the study area is controlled by the sign and magnitude of relative errors at the census block level. Since underestimation usually happens in census blocks with high population density, the total population count in the study

area is underestimated, with a minimum estimation error of about -6%. Median relative estimation error at block level for the regression models range from 13.6% to 20.3%. Such accuracy is not high enough for small area population estimation. Possible reason behind the relatively low accuracies could be the lack of high resolution LiDAR data. It would be interesting to compare the results with those derived from high resolution LiDAR data. Alternative models such as kriging should be evaluated to address issues caused by small numbers and variations in the population density.

REFERENCES

Alexander, C., Voysey, S.S., Jarvis, C., Tansey, K. (2009). Integrating building footprints and LiDAR elevation data to classify roof structures and visualise buildings. *Computers, Environment and Urban Systems*, *33*, 285-292.

Antonarakis, A.S., Richards, K.S., Brasington, J. (2008). Object-based land cover classification using airborne LiDAR. *Remote Sensing of Environment*, *112*, 2988-2998.

Aubrecht, C., Steinnocher, K., Hollaus, M., Wagner, W. (2009). Integrating earth observation and GIScience for high resolution spatial and functional modeling of urban land use. *Computers, Environment and Urban Systems*, *33*, 15-25.

Baatz, M., Benz, U., Dehghani, S., Heynen, M., Höltje, A., Hofmann, P., Lingenfelder, I., Mimler, M., Sohlbach, M., Weber, M., Willhauck, G. (2004). *eCognition user guide 4*. Germany: Definiens Imaging.

Blaschke, T. (2003). Object-based contextual image classification built on image segmentation. *Advances in Techniques for Analysis of Remotely Sensed Data, 34*, 113-119.

Bork, E.W., Su, J.G. (2007). Integrating LIDAR data and multispectral imagery for enhanced classification of rangeland vegetation: A meta analysis. *Remote Sensing of Environment*, *111*, 11-24.

Briggs, D.J., Gulliver, J., Fecht, D., Vienneau, D.M. (2007). Dasymetric modelling of small-area population distribution using land cover and light emissions data.*Remote Sensing of Environment*, *108*, 451-466.

Carter, J.R. (1988). Digital representation of topographic surfaces. P*hotogrammetric Engineering and Remote Sensing*, *54*, 1551-1555.

Chen, K. (2002). An approach to linking remotely sensed data and areal census data. *International Journal of Remote Sensing*, *23*, 37-48.

Chen, Y., Su, W., Li, J., Sun, Z. (2008). Hierarchical object oriented classification using very high resolution imagery and LIDAR data over urban areas. *Advances in Space Research, 43*, 1101-1110.

Clement, F., Orange, D., Williams, M., Mulley, C., & Epprecht, M. (2009). Drivers of afforestation in Northern Vietnam: Assessing local variations using

geographically weighted regression. *Applied Geography*, *29*(4), 561-576.

Darwish, A., Leukert, K., Reinhardt, W. (2003). Urban land-cover classification: an object based perspective. *Proceedings of the 2nd GRSS/ISPRS Joint Workshop on Data Fusion and Remote Sensing over Urban Areas,* 278-282.

Dehvari, A., Heck, R. J. (2009). Comparison and object-based and pixel based infrared airborne image classification methods using DEM thematic layer. *Journal of Geography and Regional Planning*, *2*(4), 086-096.

Dong, P. (2009). Characterization of individual tree crowns using three-dimensional shape signatures derived from LiDAR data. *International Journal of Remote Sensing*. (in press).

Gao, Y., Mas, J.F., & Navarrete, A. (2009). The improvement of an object-oriented classification using multi-temporal MODIS EVI satellite data. *International Journal of Digital Earth, 2*(3), 219-236.

George, H.C., Charalampidis, D., Alphonso, K. (2008, March). Determination of building footprints from LIDAR data. *Proceedings of the 40th Southeastern Symposium on Systems Theory, 132-136.*

Haala, N., Brenner, C. (1999). Extraction of buildings and trees in urban environments. *ISPRS Journal of Photogrammetry and Remote Sensing*, *54*, 130-137.

Hardin, P.J., Jackson, M.W., Shumway, J.M. (2007). Intraurban population estimation using remotely sensed imagery. *Geo-spatial technologies in urban environment* (pp. 47-92). Heidelburg, Berlin: Springer.

Harvey, J.T. (2002a). Estimating census district populations from satellite imagery: Some approaches and limitations. *International Journal of Remote Sensing*, *23*, 2071-2095.

Henderson, F. M., & Zong-Guo Xia. (1997). SAR applications in human settlement detection, population estimation and urban land use pattern analysis: A status report. *Geoscience and Remote Sensing, IEEE Transactions*, *5*(1), 79-85.

Koc, D., Turker, M. (2005). Automatic building detection from high resolution satellite images. *Recent Advances in Space Technologies*, *43*, 617- 622.

Li, G., Weng, Q. (2005). Using Landsat ETM+ imagery to measure population density in Indianapolis, Indiana, USA. *Photogrammetric Engineering and Remote Sensing*, *71*, 947-958.

Lillesand, T. M., Kiefer, R. W., Chipman, J. W. (2004). *Remote sensing and image interpretation*. New Jersey, NJ: John Wiley & sons.

Lo, C.P. (1986). Accuracy of population estimation from medium-scale aerial photography. *Photogrammetric Engineering & Remote Sensing*, *52*, 1859-1869.

Lo, C.P. (1995). Automated population and dwelling unit estimation from high-resolution satellite images: A GIS approach. *International Journal of Remote Sensing*, *16*, 17-34.

Lu, D., Weng, Q., Li, G. (2006). Residential population estimation using a remote sensing derived impervious surface approach*. International Journal of Remote Sensing*, *27*, 3553-3570.

Maas, H.G., Vosselman, G. (1999). Two algorithms for extracting building models from raw laser altimetry data. *ISPRS Journal of Photogrammetry and Remote Sensing*, *54*, 153-163.

Matei, B.C., Sawhney, H.S., Samarasekera, S., Kim, J., Kumar, R. (2008). Building segmentation for densely built urban regions using aerial LIDAR data. *Computer Vision and Pattern Recognition*, *12*, 1-8.

Michaelsen, E., Thiele, A., Cadario, E., & Soergel, U. (2008). Building extraction based on stereo analysis of high-resolution SAR images taken from orthogonal aspect directions. *Pattern Recognition and Image Analysis*, *18*(2), 231-235.

Ogneva-Himmelberger, Y., Pearsall, H., & Rakshit, R. (2009). Concrete evidence & geographically weighted regression: A regional analysis of wealth and the land cover in Massachusetts*. Applied Geography*, *29*(4), 478-487.

Olorunfemi, J.F. (1984). Land use and population: A linking model. *Photogrammetric Engineering and Remote Sensing*, *50*, 221-227.

Porter P.W., 1956. *Population distribution and land use in Liberia*, Ph.D. dissertation, London School of Economics and Political Science, London.

Qiu, F., Woller, K.L., Briggs, R. (2003). Modeling urban population growth using remotely sensed imagery and TIGER GIS road data. *Photogrammetric Engineering & Remote Sensing*, *69*, 1031-1042.

Rottensteiner, F., Briese, C. (2003). Automatic generation of building models from LiDAR data and integration of aerial images. *International Archives of Photogrammetry and Remote Sensing*, *34*, 174-180.

Sims, F.M., Mesev, V. (2007). Use of ancillary data in object based classification of high resolution satellite data. *Urban Remote Sensing*, *1*, 1-10.

Smith, S. K., and Cody, S. (1994). Evaluating the housing unit method: A case study of 1990 population estimates in Florida. *Journal of the American Planning Association*, *60*, 209-221.

Smith, S. K., and Lewis, B. (1980). Some new techniques for applying the housing unit method of local population estimation. *Demography*, *17*, 323-339.

Stow, D., Lopez, A., Lippit, C., Hinton, S., and Weeks, J. (2007). Object-based classification of residential land use within Accra, Ghana based on Quickbird satellite data. *International Journal of Remote Sensing*, *28*, 5167-5173.

Suveg, I., Vosselman, G. (2004). Reconstruction of 3D building models from aerial images and maps*. ISPRS Journal of Photogrammetry and Remote Sensing*, *58*, 202-224.

Vosselman, G., Kessels, P., Gorte, B. (2005). The utilisation of airborne laser scanning for mapping*. International Journal of Applied Earth Observation and Geoinformation*, *6*, 177-186.

Vu, Thuy, T., Yamazaki, F., and Matsuoka, M. (2009). Multi-scale solution for building extraction from LiDAR and image data. *International Journal of Applied Earth Observation and Geoinformation*, *11*(4), 281-289.

Weber, C. (1994). Per-zone classification of urban land use cover for urban population estimation. *Environmental Remote Sensing from Regional to Global Scales*, *45*, 142-148.

Wu, C., and Murray, A. T. (2005). A cokriging method for estimating population density in urban areas. *Computers, Environment and Urban Systems*, *29*, 558-579.

Wu, S., Qiu, X., Wang, L. (2005). Population estimation methods in GIS and remote sensing: A review. *GIScience and Remote Sensing*, *42*, 58-74.

Zeng, Q., Lai, J., Li, X., Mao, J., Liu, X. (2008). Simple building reconstruction from LIDAR point cloud. *Audio, Language and Image Processing*, *10*, 1040-1044.

Zhou, G., Song, C., Simmers, J., Cheng, P. (2004). Urban 3D GIS from LiDAR and digital aerial images. *Computers & Geosciences*, *30*, 345-353.